

## CLIMATOLOGY

# Limited contribution of ancient methane to surface waters of the U.S. Beaufort Sea shelf

Katy J. Sparrow,<sup>1,2\*</sup> John D. Kessler,<sup>1\*</sup> John R. Southon,<sup>3</sup> Fenix Garcia-Tigreros,<sup>1</sup> Kathryn M. Schreiner,<sup>4,5</sup> Carolyn D. Ruppel,<sup>6</sup> John B. Miller,<sup>7,8</sup> Scott J. Lehman,<sup>9</sup> Xiaomei Xu<sup>3</sup>

In response to warming climate, methane can be released to Arctic Ocean sediment and waters from thawing subsea permafrost and decomposing methane hydrates. However, it is unknown whether methane derived from this sediment storehouse of frozen ancient carbon reaches the atmosphere. We quantified the fraction of methane derived from ancient sources in shelf waters of the U.S. Beaufort Sea, a region that has both permafrost and methane hydrates and is experiencing significant warming. Although the radiocarbon-methane analyses indicate that ancient carbon is being mobilized and emitted as methane into shelf bottom waters, surprisingly, we find that methane in surface waters is principally derived from modern-aged carbon. We report that at and beyond approximately the 30-m isobath, ancient sources that dominate in deep waters contribute, at most,  $10 \pm 3\%$  of the surface water methane. These results suggest that even if there is a heightened liberation of ancient carbon-sourced methane as climate change proceeds, oceanic oxidation and dispersion processes can strongly limit its emission to the atmosphere.

## INTRODUCTION

Methane ( $\text{CH}_4$ ) emissions from Arctic Ocean shelf seas are anomalously large relative to those of the global mean ocean (1–4), but the source of these emissions remains largely unknown. Permafrost, which contains perennially frozen ancient carbon (C) (5), and  $\text{CH}_4$  hydrate, an ice-like form of  $\text{CH}_4$  that is principally ancient and older than surrounding sediment (6), are often invoked as likely sources because both constitute large C reservoirs and can be converted to  $\text{CH}_4$  gas as a result of warming climate. Although the global atmospheric  $\text{CH}_4$  inventory is increasing, arctic  $\text{CH}_4$  growth rates are comparable to or less than the global average (7) and appear to be derived mainly from biogenic sources (2, 8, 9). Ancient C stores, including arctic permafrost and hydrates, were recently determined to have contributed  $\leq 19\%$  of the  $\text{CH}_4$  released to the atmosphere during the Younger Dryas–Preboreal abrupt warming event (10), an analog to climate change today. Because of residual, fundamental unknowns about  $\text{CH}_4$  emissions from permafrost and hydrates, this potentially catastrophic climatological feedback has been absent from most Earth system models (5, 11).

Previous studies of  $\text{CH}_4$  dynamics in Arctic Ocean continental margins have measured atmospheric  $\text{CH}_4$  mole fractions ( $[\text{CH}_4]$ ), dissolved  $[\text{CH}_4]$ , and dissolved stable C isotopes ( $\delta^{13}\text{C-CH}_4$ ) to document emissions from the seafloor to the water column and from the water column to the atmosphere (1–4, 12–16). Because no study has conclusively fingerprinted the source of this  $\text{CH}_4$ , it is unknown what fraction emitted to the atmosphere from the shallow arctic shelf seas is derived from ancient C sources. These ancient C  $\text{CH}_4$  sources are terrestrial and

subsea permafrost via the biological transformation of thawed organic C (5), subsea permafrost-associated  $\text{CH}_4$  hydrates (6), and geologic  $\text{CH}_4$ . Methane sources to seawater derived from modern-aged C include the atmosphere (17) and in situ production from more modern-aged substrates (12, 18).

Ancient and modern C-sourced  $\text{CH}_4$  can be readily distinguished with natural abundance  $^{14}\text{C-CH}_4$  measurements, as radioactive decay leaves ancient C sources substantially depleted in  $^{14}\text{C}$  with respect to modern C sources. Thermonuclear weapons and nuclear power generation have introduced anthropogenic  $^{14}\text{C}$  into atmospheric and oceanic  $\text{CH}_4$  (17, 19). We collected dissolved  $^{14}\text{C-CH}_4$  samples to test the hypotheses that (i) ancient C sources contribute  $\text{CH}_4$  to Arctic Ocean continental shelf waters and (ii) the contribution of ancient C sources to surface water and atmospheric  $\text{CH}_4$  in this environment diminishes as proximity to these sources decreases (that is, as water depth and distance from shore increase). Without newly developed techniques (Materials and Methods) (20), testing these hypotheses would not have been possible due to the challenge of collecting sufficient quantities of  $\text{CH}_4$  for natural abundance  $^{14}\text{C-CH}_4$  analysis in surface waters (1, 3, 4, 12, 13, 15, 16).

## RESULTS AND DISCUSSION

The continental shelf offshore Prudhoe Bay, AK, in the U.S. Beaufort Sea was chosen as an ideal site to assess the input of ancient C-sourced  $\text{CH}_4$  to surface waters (Fig. 1A). Figure 1B illustrates the components of the Prudhoe Bay system schematically, including  $^{14}\text{C}$  measurements of dissolved  $\text{CH}_4$  and possible ancient and modern endmembers. The seaward extent of persistent subsea ice-bonded permafrost in this shelf sea, which was unglaciated land during the Late Pleistocene, has been determined from seismic reflection analysis (21) and verified with direct evidence from borehole well data (Fig. 1A) (22). Gas hydrates may occur within and beneath permafrost in this passive margin shelf (22) and may dissociate to release  $\text{CH}_4$  even after the permafrost matrix has thawed (6). Terrestrial peat and permafrost soils (5, 23, 24), including yedoma permafrost (25), are other potential sources of ancient  $\text{CH}_4$  delivered to the shelf by rivers [mainly the Colville and Mackenzie rivers (24)], coastal erosion, and submarine groundwater discharge

Copyright © 2018  
The Authors, some  
rights reserved;  
exclusive licensee  
American Association  
for the Advancement  
of Science. No claim to  
original U.S. Government  
Works. Distributed  
under a Creative  
Commons Attribution  
NonCommercial  
License 4.0 (CC BY-NC).

<sup>1</sup>Department of Earth and Environmental Sciences, University of Rochester, Rochester, NY 14627, USA. <sup>2</sup>Department of Environmental Science and Analytical Chemistry, Bolin Centre for Climate Research, Stockholm University, Stockholm, Sweden. <sup>3</sup>Keck Carbon Cycle Accelerator Mass Spectrometry Laboratory, Department of Earth System Science, University of California, Irvine, Irvine, CA 92697, USA. <sup>4</sup>Large Lakes Observatory, University of Minnesota Duluth, Duluth, MN 55812, USA. <sup>5</sup>Department of Chemistry and Biochemistry, University of Minnesota Duluth, Duluth, MN 55812, USA. <sup>6</sup>U.S. Geological Survey, Woods Hole, MA 02543, USA. <sup>7</sup>Cooperative Institute for Research in Environmental Sciences, University of Colorado Boulder, Boulder, CO 80309, USA. <sup>8</sup>Global Monitoring Division, Earth System Research Laboratory, National Oceanic and Atmospheric Administration, Boulder, CO 80305, USA. <sup>9</sup>Institute of Arctic and Alpine Research, University of Colorado Boulder, Boulder, CO 80309, USA.  
\*Corresponding author. Email: katysparrow@gmail.com (K.J.S.); john.kessler@rochester.edu (J.D.K.)

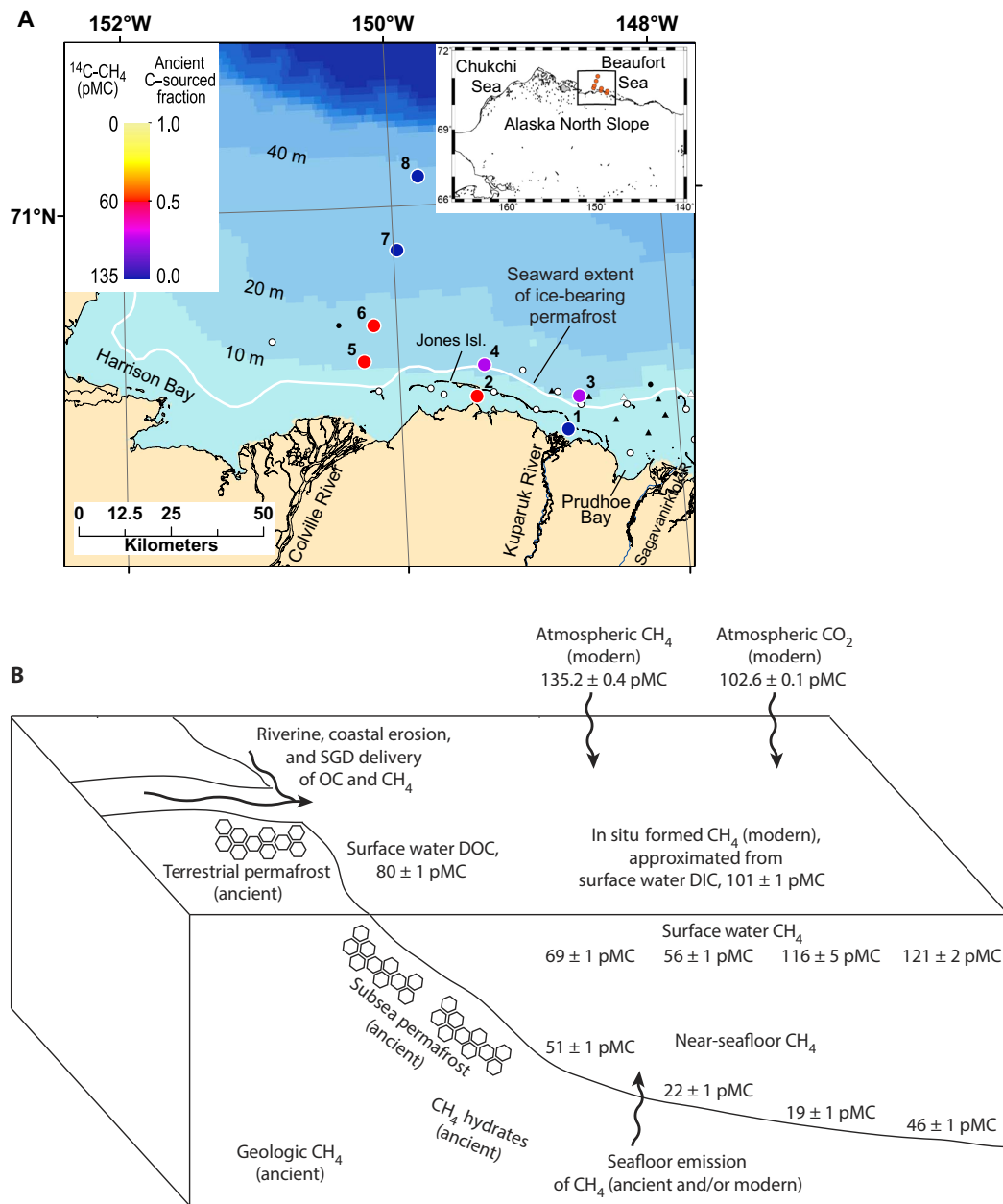


**Fig. 1. Surface water  $^{14}\text{C-CH}_4$  data and potential  $\text{CH}_4$  endmembers in the U.S. Beaufort Sea shelf study area.** (A) Station map showing both the  $^{14}\text{C-CH}_4$  data in units of percent Modern Carbon (pMC), with the atmosphere in 1950 defined as 100 pMC (33, 34), as well as the calculated fraction of ancient C-sourced  $\text{CH}_4$  ( $f$ ) (Eqs. 1 to 5) in surface waters at each station. The white curve is the bulk sediment velocity contour (2000 m/s) used to delineate the seaward boundary of the sedimentary section that contains substantial (up to 29%) ice-bearing permafrost in the upper ~600 m (21). White circles and triangles respectively show boreholes (hundreds of meters deep) and geotechnical borings (<100 m) that contain permafrost based on an analysis of well logs and recovery of permafrost samples, respectively (22). Black circles and triangles respectively indicate no permafrost inferred or found in deep boreholes and geotechnical borings (22). (B) System schematic showing  $^{14}\text{C}$  values of dissolved  $\text{CH}_4$  (stations 5 to 8) and possible ancient and modern endmembers that were also measured here. SGD, submarine groundwater discharge; OC, organic carbon; DOC, dissolved organic carbon.

(26) (Fig. 1B). Rates of both terrestrial permafrost degradation near the Colville River and erosion along the area's permafrost-dominated coastline have been increasing in recent years (27, 28). Atmospheric  $\text{CH}_4$  in this system (and globally, as described above) has a  $^{14}\text{C}$  activity above modern because the atmosphere is both the site of natural  $^{14}\text{C}$  production and influenced by  $^{14}\text{C}$ -enriched  $\text{CH}_4$  produced by nuclear reactors (17). A second modern  $\text{CH}_4$  source in the system is in situ

aerobic methanogenesis associated with the production and decomposition of phytoplankton biomass (12, 18), which we assume is similar to the measured  $^{14}\text{C}$  content of dissolved inorganic carbon (DIC) in surface waters (Fig. 1B). Anaerobic methanogenesis from the metabolism of recently fixed organic matter in sediment (29) is also a potential source of modern methane, but the substrate must be modern and not from one of the ancient C sources highlighted above. For this reason,

we assume that this third potential modern  $\text{CH}_4$  source has a  $^{14}\text{C}$  content similar to that of DIC in surface waters (Fig. 1B).

Although these disparate sources can contribute  $\text{CH}_4$  to the Beaufort Sea shelf (Fig. 1B), a plot of  $^{14}\text{C-CH}_4$  versus the reciprocal of molar  $[\text{CH}_4]$ , a so-called Keeling plot (30, 31), displays surprising linearity for a complex system ( $R^2 = 0.75$ ) (Fig. 2). The relationship is statistically significant ( $P < 0.01$ ) and suggests that the observed (“obs”) system can be largely described as a mixture of modern background (“bkg”) and an ancient source (“s”); this result does not exclude the possibility that multiple sources of  $\text{CH}_4$  may contribute to the source and/or the background values, but it does suggest that potential  $\text{CH}_4$  endmembers can be linearly combined to establish a pseudo–two-component mixture

$$c_{\text{obs}} = c_{\text{bkg}} + c_s \quad (1)$$

$$^{14}\text{C}_{\text{obs}} c_{\text{obs}} = ^{14}\text{C}_{\text{bkg}} c_{\text{bkg}} + ^{14}\text{C}_s c_s \quad (2)$$

where “c” is  $[\text{CH}_4]$  and “ $^{14}\text{C}$ ” is  $^{14}\text{C-CH}_4$  content. Combining and rearranging Eqs. 1 and 2 yields a linear equation (Eq. 3), whose  $y$  intercept indicates the  $^{14}\text{C-CH}_4$  content of the source ( $^{14}\text{C}_s$ ) when an infinite amount of source is added (Fig. 2B) (30).

$$^{14}\text{C}_{\text{obs}} = c_{\text{bkg}}(^{14}\text{C}_{\text{bkg}} - ^{14}\text{C}_s)(1/c_{\text{obs}}) + ^{14}\text{C}_s \quad (3)$$

Because the values of both  $^{14}\text{C}_{\text{obs}}$  and  $1/c_{\text{obs}}$  contain uncertainty, a standard Model I, linear least squares regression, is inappropriate to determine the  $y$  intercept; instead, a Model II, geometric mean regression, is often preferred (31, 32). This analysis is used here (Fig. 2B) and suggests that  $^{14}\text{C}_s$  equals  $-5.60 \pm 11.22$  percent Modern Carbon (pMC) relative to the 1950 atmosphere, which is defined as 100 pMC (33, 34). Negative values of pMC have no meaning, so  $^{14}\text{C}_s$  likely ranges from 0 to 5.62 pMC, indicating that ancient sources of  $\text{CH}_4$  (zero to low  $^{14}\text{C}$  content,

$<<100$  pMC) (Fig. 1B) are being added to the background  $\text{CH}_4$  in these waters. Although this analysis cannot distinguish between different ancient sources of  $\text{CH}_4$ , it does suggest that at least one, if not several, of the ancient sources is contributing  $\text{CH}_4$  to this region, confirming previous conjectures (5, 6, 13–16). The background  $\text{CH}_4$  to which these ancient sources are added is likely composed of more modern  $\text{CH}_4$  ( $\geq 100$  pMC) from the atmosphere ( $135.2 \pm 0.4$  pMC;  $n = 3$ ), in situ aerobic (water column) and anaerobic (sediment) methanogenesis ( $101 \pm 1$  pMC;  $n = 6$ ), or some combination of the three (Fig. 1B).

We calculate the fraction of each dissolved  $\text{CH}_4$  sample that was derived from the ancient C source ( $f_s$ ) with an isotopic mass balance

$$^{14}\text{C}_{\text{obs}} = ^{14}\text{C}_h(f_h) + ^{14}\text{C}_p(f_p) + ^{14}\text{C}_a(f_a) + ^{14}\text{C}_i(f_i) \quad (4)$$

$$1 = f_h + f_p + f_a + f_i \quad (5)$$

where the radiocarbon content of each  $\text{CH}_4$  endmember is represented by the subscripts “h” (hydrate or geologic  $\text{CH}_4$ ; 0 pMC), “p” (permafrost  $\text{CH}_4$ ; 5.62 pMC), “a” (atmospheric  $\text{CH}_4$ ; 135.2 pMC), and “i” (in situ produced  $\text{CH}_4$ ; 101 pMC) (Fig. 1). Because this isotopic mass balance contains two equations and four unknowns ( $f_h, f_p, f_a$ , and  $f_i$ ), we begin by defining  $f_a$  and  $f_i$  by systematically varying them from 0 to 1 in increments of 0.001, considering all possible combinations. Then, values of  $f_h$  and  $f_p$  are calculated using Eqs. 4 and 5 for each unique combination of  $f_a$  and  $f_i$ . When either  $f_h$  or  $f_p$  is determined to be less than 0 or greater than 1, all values are discarded for that linear combination. The resulting values of  $f_h$  and  $f_p$  are summed to more generally represent  $f_s$  because  $^{14}\text{C}_h$  and  $^{14}\text{C}_p$  are assumed on the basis of the results of the Keeling plot (Fig. 2B) and not directly measured; the average and standard deviation of  $f_s, f_a$ , and  $f_i$  are then calculated (Table 1 and Fig. 1A).

In the back-barrier lagoon (stations 1 and 2), where sediment overlies intact subsea permafrost (Fig. 1A) (21, 22), just one “lagoon”  $^{14}\text{C-CH}_4$  sample was collected per station because of the shallow water depth ( $< 3$  m) (Fig. 2A). At each of the six deeper-water stations

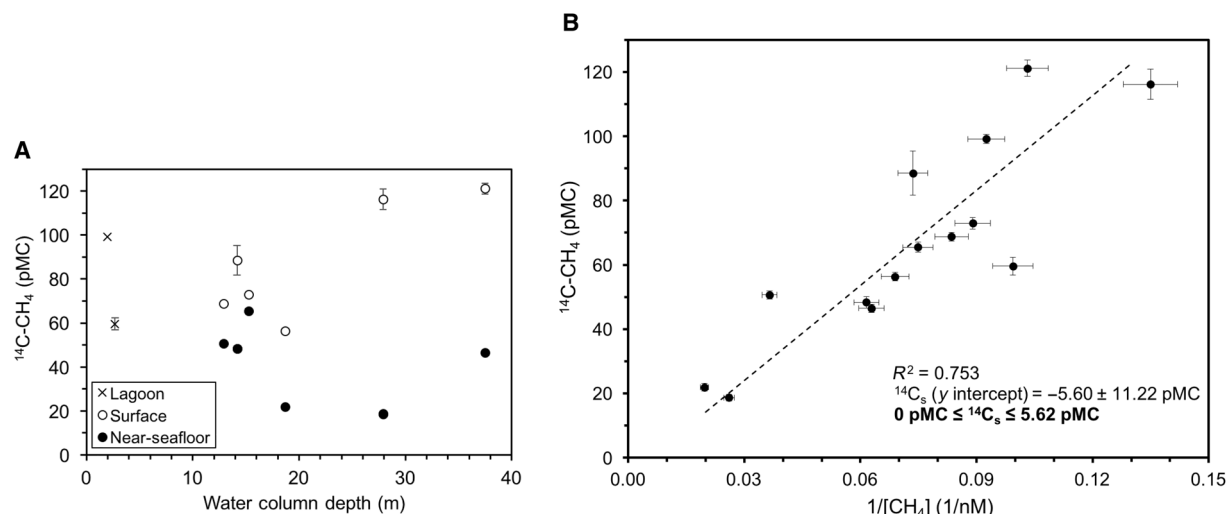


**Fig. 2.**  $^{14}\text{C-CH}_4$  data from each station and Keeling plot analysis. **(A)** Dissolved  $^{14}\text{C-CH}_4$  data for stations 1 to 8, plotted by the water depth of the station. The data include lagoon samples (x), surface samples (white circles), and near-seafloor samples (black circles). Error bars that are not visible are smaller than the markers. Uncertainty for  $^{14}\text{C-CH}_4$  data incorporates the collection, preparation, and measurement uncertainties (20). **(B)** A Keeling plot (Eq. 3) incorporating  $[\text{CH}_4]$  and  $^{14}\text{C-CH}_4$  measurements from stations 1 to 8 suggests that the system can be viewed as a pseudo–two-component mixture and that the  $^{14}\text{C-CH}_4$  source signature ( $^{14}\text{C}_s$ ) likely ranges from 0 to 5.62 pMC.

**Table 1. Calculated fractions of ancient and modern C-sourced  $\text{CH}_4$  in each sample.**

Station	Water depth (m)	Distance offshore (km)	Sample type	Ancient C-sourced $\text{CH}_4$ fraction, $f_s$	Atmospheric-sourced $\text{CH}_4$ fraction, $f_a$	In situ produced $\text{CH}_4$ fraction, $f_i$
1	2	3	Lagoon	0.18 ± 0.06	0.47 ± 0.18	0.35 ± 0.25
2	3	2	Lagoon	0.50 ± 0.04	0.23 ± 0.12	0.27 ± 0.17
3	14	12	Surface	0.26 ± 0.06	0.37 ± 0.18	0.37 ± 0.24
			Near-seafloor	0.60 ± 0.04	0.18 ± 0.10	0.22 ± 0.13
4	15	10	Surface	0.39 ± 0.05	0.29 ± 0.15	0.33 ± 0.20
			Near-seafloor	0.45 ± 0.05	0.25 ± 0.14	0.30 ± 0.18
5	13	18	Surface	0.42 ± 0.05	0.27 ± 0.14	0.31 ± 0.19
			Near-seafloor	0.58 ± 0.04	0.19 ± 0.10	0.23 ± 0.14
6	19	27	Surface	0.53 ± 0.04	0.21 ± 0.12	0.26 ± 0.16
			Near-seafloor	0.83 ± 0.02	0.07 ± 0.04	0.10 ± 0.06
7	28	48	Surface	0.10 ± 0.03	0.72 ± 0.10	0.18 ± 0.13
			Near-seafloor	0.86 ± 0.02	0.06 ± 0.04	0.08 ± 0.05
8	38	69	Surface	0.07 ± 0.03	0.79 ± 0.07	0.14 ± 0.10
			Near-seafloor	0.61 ± 0.03	0.17 ± 0.10	0.22 ± 0.13

(stations 3 to 8), two  $^{14}\text{C}$ - $\text{CH}_4$  samples were collected: a “surface” sample acquired at 2 m below the sea surface and a “near-seafloor” sample collected 3 to 8 m from the seafloor (table S1 and Fig. 2A).

The  $\delta^{13}\text{C}$ - $\text{CH}_4$  and  $[\text{CH}_4]$  data associated with each  $^{14}\text{C}$ - $\text{CH}_4$  sample are presented in table S1. The average values for the surface samples ( $-58 ± 6\text{‰}$ ,  $11 ± 3 \text{ nmol/liter (nM)}$ ;  $n = 6$ ) are more enriched in  $^{13}\text{C}$  and have lower concentrations than those of the near-seafloor samples ( $-63 ± 6\text{‰}$ ,  $27 ± 15 \text{ nM}$ ;  $n = 6$ ). These observations are also true of each station’s surface and near-seafloor pair (fig. S1). Because  $^{12}\text{CH}_4$  is oxidized faster than  $^{13}\text{CH}_4$ , these trends support the traditional view of oceanic  $\text{CH}_4$  dynamics, in which  $\text{CH}_4$  is emitted from anoxic seafloor sediments and oxidized throughout its ascent in the water column (35).

In sharp contrast, the values of  $f_s$  computed from the  $^{14}\text{C}$ - $\text{CH}_4$  data allow an entirely different interpretation of this system. The lagoon sample collected at station 1 is composed mainly of modern background  $\text{CH}_4$  ( $f_s = 0.18 ± 0.06$ ), whereas the sample collected from station 2 is of intermediate origin ( $f_s = 0.50 ± 0.04$ ), a roughly equivalent mixture of ancient C source and modern background. The mean value of  $f_s$  in the near-seafloor samples ranges from 0.45 to 0.86 ( $n = 6$ ), whereas the mean value of  $f_s$  in the surface samples ranges from 0.07 to 0.53 ( $n = 6$ ). The surface samples are all dominantly modern background  $\text{CH}_4$  except for the sample collected at station 6, which has an intermediate origin ( $f_s = 0.53 ± 0.04$ ).

At stations 3, 5, 7, and 8,  $\text{CH}_4$  in the near-seafloor sample is derived mainly from ancient C sources in contrast to  $\text{CH}_4$  derived mainly from modern background in the surface water sample. This decoupling is most evident at mid-outer shelf stations 7 and 8 (at water depths of 28 and 38 m, respectively), where little to no  $\text{CH}_4$  is sourced from ancient C in surface waters, whereas  $\text{CH}_4$  found near the seafloor is mainly sourced from ancient C (Table 1). These analyses suggest that (i) ancient C sources supply  $\text{CH}_4$  to shelf waters and (ii) ancient C sources contrib-

ute little to no  $\text{CH}_4$  to surface waters (and therefore to the atmosphere) with increasing water depth and thus confirms our hypotheses.

These results demonstrate that ancient C-sourced  $\text{CH}_4$  offshore Prudhoe Bay is largely not reaching the atmosphere beyond, approximately, the 30-m isobath. Our findings are consistent with other Arctic Ocean studies that have found  $\text{CH}_4$  removal processes to be highly efficient in sediment (36) and relatively shallow water columns ( $<100 \text{ m}$  depth) (15, 16). The evidence of strong  $\text{CH}_4$  removal mechanisms operating in the Arctic from these studies suggests that an enhancement of ancient C mobilization due to climate change would not necessarily increase  $\text{CH}_4$  emission to the atmosphere from the Arctic Ocean. In addition to potential changes in the magnitude of  $\text{CH}_4$  sources in a warmer, increasingly ice-free Arctic Ocean (37), we must also consider that the rate of  $\text{CH}_4$  removal processes, such as aerobic  $\text{CH}_4$  oxidation by microorganisms in the water column (6, 35), could also change. Thus, to accurately constrain the mobilization of ancient C and the subsequent emission of  $\text{CH}_4$ , we recommend that natural abundance  $^{14}\text{C}$ - $\text{CH}_4$  analyses should be conducted in future studies of  $\text{CH}_4$  dynamics.

## MATERIALS AND METHODS

### Sample collection

Our study was carried out aboard the R/V *Ukpiq* from 30 August to 5 September 2015, coincident with the period of the year that typically has the minimum extent of sea ice. Because the surface water  $[\text{CH}_4]$  in the Prudhoe Bay area is lower than the limit of previous  $^{14}\text{C}$ - $\text{CH}_4$  techniques (16 nM for a small sample accelerator mass spectrometry analysis) (38), a new dissolved  $^{14}\text{C}$ - $\text{CH}_4$  sampling and preparation method was developed and used in this study (20). Using this method, seawater was continuously pumped onboard and the dissolved gases were continuously extracted from the water. In the Prudhoe Bay sample set,

the average seawater sample volume was  $32,000 \pm 4000$  liters ( $n = 14$ ), and the average extracted gas volume was  $350 \pm 50$  liters ( $n = 14$ ). The extracted gas was compressed into a 2-liter cylinder for transport to the home laboratory, where it was prepared for  $^{14}\text{C}$  and stable isotope analyses. Although the cylinder is only pressurized to a maximum of 2100 psi, equivalent to 240 liters, it was necessary to extract 350 to 400 liters of gas to (i) flush the compressor pump and cylinder with sample and (ii) account for some small, unresolved loss of sample (that is, a leak) in the compression process.

Atmospheric  $\text{CH}_4$  for  $^{14}\text{C-CH}_4$  analyses was sampled in Utqiagvik (formerly, Barrow), AK, on three separate days across 3 months (August to October 2015, bounding our cruise dates) and is reported as mean  $\pm 1$  SD ( $n = 3$ ); the samples were collected when winds were coming from the north, so these measurements represent a circum-Arctic average, to some extent. Atmospheric  $\text{CO}_2$  for  $^{14}\text{C-CO}_2$  analyses was also sampled in Utqiagvik, AK, on three separate days across 3 weeks (August to September 2015, bounding our cruise dates) and is reported as mean  $\pm 1$  SD ( $n = 3$ ). DIC and DOC samples for  $^{14}\text{C-DIC}$  and  $^{14}\text{C-DOC}$  analyses were collected contemporaneously with  $^{14}\text{C-CH}_4$  sampling on our research cruise; these measurements are reported as the mean  $\pm 1$  SD of surface water samples (2 m depth) at stations 3 to 8 ( $n = 6$ ).

A discrete vial for  $[\text{CH}_4]$  analysis was collected at each sample collection depth using a single Niskin bottle following standardized procedures (39). In total, 16 samples were collected from the 14 sample collection depths because two duplicate vials were collected. Each sample was collected by transferring the seawater in the Niskin bottle to a 60-ml glass vial, which was flushed with seawater, filled, and sealed with a stopper and crimp cap. Then, a 10-ml gaseous headspace of ultrahigh-purity nitrogen was injected into each vial from a syringe while 10 ml of seawater from the vial was removed with a second syringe. Each sample was then sterilized with 25  $\mu\text{l}$  of supersaturated mercuric chloride solution to prevent microbial perturbation of the original  $[\text{CH}_4]$  and stored stopper side down to prevent any diffusion of headspace gas across the seal.

The  $[\text{CH}_4]$  analyses were performed 2 months after the cruise in the home laboratory using an Agilent 6850 gas chromatograph with a flame ionization detector (GC-FID). The GC analysis of the headspace of each vial was performed in two consecutive runs. The  $[\text{CH}_4]$  of the headspace was calculated by fitting the measured peak area to a four-point calibration curve created on the same day by analyzing a suite of  $\text{CH}_4$  gas standards  $\{[\text{CH}_4] = 0, 1, 10, \text{ and } 100 \text{ parts per million (ppm)}\}$  that bound all of the measured values. The measured headspace  $[\text{CH}_4]$  of each vial was translated to a dissolved  $[\text{CH}_4]$  value (40) with knowledge of the sample incubator temperature and the salinity of the sampled seawater, the latter of which was measured with a water quality sonde in the field (YSI, 600R series). An uncertainty of 5.2% is associated with each measurement (39).

To evaluate the degree of  $\text{CH}_4$  saturation in the sampled seawater from the dissolved  $[\text{CH}_4]$  data, it was necessary to calculate the  $[\text{CH}_4]$  that would be found if each water sample had come to full equilibrium with the atmosphere (that is, the “equilibrium solubility”). The local atmosphere was sampled from bow air that was pumped to an onboard cavity ring-down spectrometer (CRDS; G2401, Picarro). The atmospheric  $[\text{CH}_4]$  ( $2.000 \pm 0.002 \text{ ppm}$ ;  $n = 79$ ) was used along with the temperature- and salinity-dependent  $\text{CH}_4$  solubility (40) to calculate the  $\text{CH}_4$  equilibrium solubility of each sample. The degree of  $\text{CH}_4$  saturation is reported for all surface water samples in table S1. Samples that have  $\text{CH}_4$  concentrations greater than the seawater’s

equilibrium solubility concentration have  $\text{CH}_4$  saturation values of  $>100\%$  (that is, supersaturated), representing that the net flux of  $\text{CH}_4$  is from sea to air.

### $^{14}\text{C-CH}_4$ and $\delta^{13}\text{C-CH}_4$ sample preparation

The extracted gas cylinder samples were prepared for  $^{14}\text{C-CH}_4$  and  $\delta^{13}\text{C-CH}_4$  analyses on a newly developed shore-based vacuum line (20). From 15 collected samples, 17 samples were then prepared and analyzed for  $^{14}\text{C-CH}_4$  and  $\delta^{13}\text{C-CH}_4$ , as two preparation duplicates were made by preparing a single extracted gas sample cylinder twice. Only 16 of these 17 prepared samples were analyzed (and discussed here) because a sample collected at one lagoon station (original station ID T5S29:  $70.489^\circ\text{N}$ ,  $149.114^\circ\text{W}$ ) was suspected to have been contaminated by carbon monoxide-C during the sample preparation process. The samples were prepared in a random order across 5 weeks. Vacuum line quality control assessments described by Sparrow and Kessler (20) were performed daily during the preparation period using gas standards with  $[\text{CH}_4]$  of 0, 5, and 250 ppm.

The vacuum line technique achieves high-efficiency purification, oxidation, and collection of the sample  $\text{CH}_4$ . The aliquots collected for the isotopic analyses are the  $\text{CH}_4$  oxidation products,  $\text{CO}_2$  and  $\text{H}_2\text{O}$ , which are produced when the sample  $\text{CH}_4$  is oxidized on a heated platinized quartz wool catalyst. Although the gas sample volumes are large ( $\leq 240$  liters), a high flow rate (2 liters/min) through the vacuum line allows multiple sample preparations per day. The total process blank of the procedure is small (5.0  $\mu\text{g}$  of  $\text{CH}_4\text{-C}$ ), composing 1.2% of the average collected and prepared sample ( $424 \pm 163 \mu\text{g}$ ;  $n = 16$ ). The  $^{14}\text{C-CH}_4$  blanks of the vacuum line have acceptably low radiocarbon content ( $0.22 \pm 0.07 \text{ pMC}$ ;  $n = 8$ ) relative to the  $^{14}\text{C}$ -dead (0 pMC)  $\text{CH}_4$  from which they are prepared, enabling radiocarbon dating of the dissolved  $\text{CH}_4\text{-C}$  to the analytical limit of accelerator mass spectrometry (~50,000 years Before Present).

The  $^{14}\text{C-CH}_4$  data were analyzed and corrected for isotopic fractionation (33, 34) at the W. M. Keck Carbon Cycle Accelerator Mass Spectrometry (CCAMS) Laboratory at the University of California, Irvine. The uncertainties for  $^{14}\text{C-CH}_4$  data (both  $^{14}\text{C-CH}_4$  content and conventional  $^{14}\text{C}$  age of  $\text{CH}_4$ ) reported in Fig. 1A, fig. S1, and table S1 are calculated from the root mean square of the collection, preparation, and measurement uncertainties (20). Except for two smaller-sized samples (100 and 150  $\mu\text{g}$  of  $\text{CH}_4\text{-C}$ ),  $\delta^{13}\text{C-CH}_4$  data were also analyzed at the Keck CCAMS facility to a precision of  $<0.1\%$  relative to standards traceable to Pee Dee Belemnite using a Thermo Finnigan Delta Plus stable isotope ratio mass spectrometer (IRMS) with GasBench inlet. The  $\delta^{13}\text{C-CH}_4$  measurements for the two samples that had insufficient  $\text{CH}_4\text{-C}$  for a separate IRMS aliquot were measured via CRDS (G2201-i, Picarro), analyzed directly from the sample cylinders; reported value is the 3-min average ( $n \approx 120$ ), and uncertainty is the standard error.

### SUPPLEMENTARY MATERIALS

Supplementary material for this article is available at <http://advances.sciencemag.org/cgi/content/full/4/1/eaao4842/DC1>

fig. S1. Dissolved  $\text{CH}_4$  concentration and isotopic data plotted by station depth.

table S1. Dissolved  $^{14}\text{C-CH}_4$ ,  $\delta^{13}\text{C-CH}_4$ , and  $[\text{CH}_4]$  data with relevant sample information.

### REFERENCES AND NOTES

1. B. F. Thornton, M. C. Geibel, P. M. Crill, C. Humborg, C.-M. Mört, Methane fluxes from the sea to the atmosphere across the Siberian shelf seas. *Geophys. Res. Lett.* **43**, 5869–5877 (2016).
2. A. Berchet, P. Bousquet, I. Pison, R. Locatelli, F. Chevallier, J.-D. Paris, E. J. Dlugokencky, T. Laurila, J. Hatakka, Y. Viisanen, D. E. J. Worthy, E. Nisbet, R. Fisher, J. France, D. Lowry,

V. Ivakhov, O. Hermansen, Atmospheric constraints on the methane emissions from the East Siberian Shelf. *Atmos. Chem. Phys.* **16**, 4147–4157 (2016).

3. T. D. Lorenson, J. Greinert, R. B. Coffin, Dissolved methane in the Beaufort Sea and the Arctic Ocean, 1992–2009; sources and atmospheric flux. *Limnol. Oceanogr.* **61**, S300–S323 (2016).

4. J. W. Pohlman, J. Greinert, C. Ruppel, A. Silyakova, L. Vielstädte, M. Casso, J. Mienert, S. Bünz, Enhanced CO<sub>2</sub> uptake at a shallow Arctic Ocean seep field overwhelms the positive warming potential of emitted methane. *Proc. Natl. Acad. Sci. U.S.A.* **114**, 5355–5360 (2017).

5. E. A. G. Schuur, A. D. McGuire, C. Schädel, G. Grosse, J. W. Harden, D. J. Hayes, G. Hugelius, C. D. Koven, P. Kuhry, D. M. Lawrence, S. M. Natali, D. Olefeldt, V. E. Romanovsky, K. Schaefer, M. R. Turetsky, C. C. Treat, J. E. Vonk, Climate change and the permafrost carbon feedback. *Nature* **520**, 171–179 (2015).

6. C. D. Ruppel, J. D. Kessler, The interaction of climate change and methane hydrates. *Rev. Geophys.* **55**, 126–168 (2017).

7. E. G. Nisbet, E. J. Dlugokencky, M. R. Manning, D. Lowry, R. E. Fisher, J. L. France, S. E. Michel, J. B. Miller, J. W. C. White, B. Vaughn, P. Bousquet, J. A. Pyle, N. J. Warwick, M. Cain, R. Brownlow, G. Zazzeri, M. Lanoisellé, A. C. Manning, E. Gloor, D. E. J. Worthy, E.-G. Brunke, C. Labuschagne, E. W. Wolff, A. L. Ganesan, Rising atmospheric methane: 2007–2014 growth and isotopic shift. *Global Biogeochem. Cycles* **30**, 1356–1370 (2016).

8. R. E. Fisher, S. Sriskantharajah, D. Lowry, M. Lanoisellé, C. M. R. Fowler, R. H. James, O. Hermansen, C. L. Myhre, A. Stohl, J. Greinert, P. B. R. Nisbet-Jones, J. Mienert, E. G. Nisbet, Arctic methane sources: Isotopic evidence for atmospheric inputs. *Geophys. Res. Lett.* **38**, L21803 (2011).

9. J. L. France, M. Cain, R. E. Fisher, D. Lowry, G. Allen, S. J. O'Shea, S. Illingworth, J. Pyle, N. Warwick, B. T. Jones, M. W. Gallagher, K. Bower, M. Le Breton, C. Percival, J. Muller, A. Welpott, S. Bauguitte, C. George, G. D. Hayman, A. J. Manning, C. L. Myhre, M. Lanoisellé, E. G. Nisbet, Measurements of  $\delta^{13}\text{C}$  in CH<sub>4</sub> and using particle dispersion modeling to characterize sources of Arctic methane within an air mass. *J. Geophys. Res. Atmos.* **121**, 14257–14270 (2016).

10. V. V. Petrenko, A. M. Smith, H. Schaefer, K. Riedel, E. Brook, D. Baggenstos, C. Harth, Q. Hua, C. Buzert, A. Schilt, X. Fain, L. Mitchell, T. Bauska, A. Orsi, R. F. Weiss, J. P. Severinghaus, Minimal geological methane emissions during the Younger Dryas–Preboreal abrupt warming event. *Nature* **548**, 443–446 (2017).

11. R. H. James, P. Bousquet, I. Bussmann, M. Haackel, R. Kipfer, I. Leifer, H. Niemann, I. Ostrovsky, J. Piskozub, G. Rehder, T. Treude, L. Vielstädte, J. Greinert, Effects of climate change on methane emissions from seafloor sediments in the Arctic Ocean: A review. *Limnol. Oceanogr.* **61**, S283–S299 (2016).

12. E. Damm, R. P. Kiene, J. Schwarz, E. Falck, G. Dieckmann, Methane cycling in Arctic shelf water and its relationship with phytoplankton biomass and DMSP. *Mar. Chem.* **109**, 45–59 (2008).

13. G. K. Westbrook, K. E. Thatcher, E. J. Rohling, A. M. Piotrowski, H. Pälike, A. H. Osborne, E. G. Nisbet, T. A. Minshull, M. Lanoisellé, R. H. James, V. Hühnerbach, D. Green, R. E. Fisher, A. J. Crocker, A. Chabert, C. Bolton, A. Beszczynska-Möller, C. Berndt, A. Aquilina, Escape of methane gas from the seabed along the West Spitsbergen continental margin. *Geophys. Res. Lett.* **36**, L15608 (2009).

14. N. Shakhova, I. Semiletov, V. Sergienko, L. Lobkovsky, V. Yusupov, A. Salyuk, A. Salomatin, D. Chernykh, D. Kosmach, G. Panteleev, D. Nicolsky, V. Samarkin, S. Joye, A. Charkin, O. Dudarev, A. Meluzov, O. Gustafsson, The East Siberian Arctic Shelf: Towards further assessment of permafrost-related methane fluxes and role of sea ice. *Philos. Trans. A Math. Phys. Eng. Sci.* **373**, 20140451 (2015).

15. C. A. Graves, L. Steinle, G. Rehder, H. Niemann, D. P. Connelly, D. Lowry, R. E. Fisher, A. W. Stott, H. Sahling, R. H. James, Fluxes and fate of dissolved methane released at the seafloor at the landward limit of the gas hydrate stability zone offshore western Svalbard. *J. Geophys. Res. Oceans* **120**, 6185–6201 (2015).

16. C. L. Myhre, B. Ferré, S. M. Platt, A. Silyakova, O. Hermansen, G. Allen, I. Pisso, N. Schmidbauer, A. Stohl, J. Pitt, P. Jansson, J. Greinert, C. Percival, A. M. Fjaeraa, S. J. O'Shea, M. Gallagher, M. Le Breton, K. N. Bower, S. J. B. Bauguitte, S. Dalsoren, S. Vadakkepuliyambatta, R. E. Fisher, E. G. Nisbet, D. Lowry, G. Myhre, J. A. Pyle, M. Cain, J. Mienert, Extensive release of methane from Arctic seabed west of Svalbard during summer 2014 does not influence the atmosphere. *Geophys. Res. Lett.* **43**, 4624–4631 (2016).

17. M. Wahlen, N. Tanaka, R. Henry, B. Deck, J. Zieglen, J. S. Vogel, J. Southon, A. Shemesh, R. Fairbanks, W. Broecker, Carbon-14 in methane sources and in atmospheric methane: The contribution from fossil carbon. *Science* **245**, 286–290 (1989).

18. D. J. Repeta, S. Ferrón, O. A. Sosa, C. G. Johnson, L. D. Repeta, M. Acker, E. F. DeLong, D. M. Karl, Marine methane paradox explained by bacterial degradation of dissolved organic matter. *Nat. Geosci.* **9**, 884–887 (2016).

19. J. D. Kessler, W. S. Reeburgh, D. L. Valentine, F. S. Kinnaman, E. T. Peltzer, P. G. Brewer, J. Southon, S. C. Tyler, A survey of methane isotope abundance ( $^{14}\text{C}$ ,  $^{13}\text{C}$ ,  $^2\text{H}$ ) from five nearshore marine basins that reveals unusual radiocarbon levels in subsurface waters. *J. Geophys. Res.* **113**, C12021 (2008).

20. K. J. Sparrow, J. D. Kessler, Efficient collection and preparation of methane from low concentration waters for natural abundance radiocarbon analysis. *Limnol. Oceanogr. Meth.* **15**, 601–617 (2017).

21. L. L. Brothers, B. M. Herman, P. E. Hart, C. D. Ruppel, Subsea ice-bearing permafrost on the U.S. Beaufort Margin: 1. Minimum seaward extent defined from multichannel seismic reflection data. *Geochim. Geophys. Geosyst.* **17**, 4354–4365 (2016).

22. C. D. Ruppel, B. M. Herman, L. L. Brothers, P. E. Hart, Subsea ice-bearing permafrost on the U.S. Beaufort Margin: 2. Borehole constraints. *Geochim. Geophys. Geosyst.* **17**, 4333–4353 (2016).

23. K. M. W. Anthony, P. Anthony, G. Grosse, J. Chanton, Geologic methane seeps along boundaries of Arctic permafrost thaw and melting glaciers. *Nat. Geosci.* **5**, 419–426 (2012).

24. K. M. Schreiner, T. S. Bianchi, T. I. Eglington, M. A. Allison, A. J. M. Hanna, Sources of terrigenous inputs to surface sediments of the Colville River Delta and Simpson's Lagoon, Beaufort Sea, Alaska. *J. Geophys. Res. Biogeosci.* **118**, 808–824 (2013).

25. K. M. Schreiner, T. S. Bianchi, B. E. Roseheim, Evidence for permafrost thaw and transport from an Alaskan North Slope watershed. *Geophys. Res. Lett.* **41**, 3117–3126 (2014).

26. A. L. Lecher, J. Kessler, K. Sparrow, F. Garcia-Tigreros Kodovska, N. Dimova, J. Murray, S. Tulaczyk, A. Paytan, Methane transport through submarine groundwater discharge to the North Pacific and Arctic Ocean at two Alaskan sites. *Limnol. Oceanogr.* **61**, S344–S355 (2016).

27. M. T. Jorgenson, Y. L. Shur, E. R. Pullman, Abrupt increase in permafrost degradation in Arctic Alaska. *Geophys. Res. Lett.* **33**, L02503 (2006).

28. B. M. Jones, C. D. Arp, M. T. Jorgenson, K. M. Hinkel, J. A. Schmutz, P. L. Flint, Increase in the rate and uniformity of coastline erosion in Arctic Alaska. *Geophys. Res. Lett.* **36**, L03503 (2009).

29. P. M. Crill, C. S. Martens, Methane production from bicarbonate and acetate in an anoxic marine sediment. *Geochim. Cosmochim. Acta* **50**, 2089–2097 (1986).

30. C. D. Keeling, The concentration and isotopic abundances of atmospheric carbon dioxide in rural areas. *Geochim. Cosmochim. Acta* **13**, 322–334 (1958).

31. D. E. Patakia, J. R. Ehleringer, L. B. Flanagan, D. Yakir, D. R. Bowling, C. J. Still, N. Buchmann, J. O. Kaplan, J. A. Berry, The application and interpretation of Keeling plots in terrestrial carbon cycle research. *Global Biogeochem. Cycles* **17**, 1022 (2003).

32. J. B. Miller, P. P. Tans, Calculating isotopic fractionation from atmospheric measurements at various scales. *Tellus B* **55**, 207–214 (2003).

33. M. Stuiver, H. A. Polach, Discussion reporting of  $^{14}\text{C}$  data. *Radiocarbon* **19**, 355–363 (1977).

34. S. M. Fahmi, J. R. Southon, G. M. Santos, S. W. L. Palstra, H. A. J. Meijer, X. Xu, Reassessment of the  $^{13}\text{C}/^{12}\text{C}$  and  $^{14}\text{C}/^{12}\text{C}$  isotopic fractionation ratio and its impact on high-precision radiocarbon dating. *Geochim. Cosmochim. Acta* **213**, 330–345 (2017).

35. M. Leonte, J. D. Kessler, M. Y. Kellermann, E. C. Arrington, D. L. Valentine, S. P. Sylva, Rapid rates of aerobic methane oxidation at the feather edge of gas hydrate stability in the waters of Hudson Canyon, US Atlantic Margin. *Geochim. Cosmochim. Acta* **204**, 375–387 (2017).

36. P. P. Overduin, S. Liebner, C. Knoblauch, F. Günther, S. Wetterich, L. Schirrmeyer, H.-W. Hubberten, M. N. Grigoriev, Methane oxidation following submarine permafrost degradation: Measurements from a central Laptev Sea shelf borehole. *J. Geophys. Res. Biogeosci.* **120**, 965–978 (2015).

37. J. C. Stroeve, T. Markus, L. Boisvert, J. Miller, A. Barrett, Changes in Arctic melt season and implications for sea ice loss. *Geophys. Res. Lett.* **41**, 1216–1225 (2014).

38. J. D. Kessler, W. S. Reeburgh, Preparation of natural methane samples for stable isotope and radiocarbon analysis. *Limnol. Oceanogr. Meth.* **3**, 408–418 (2005).

39. A. Weinstein, L. Navarrete, C. Ruppel, T. C. Weber, M. Leonte, M. Y. Kellermann, E. C. Arrington, D. L. Valentine, M. I. Scranton, J. D. Kessler, Determining the flux of methane into Hudson Canyon at the edge of methane clathrate hydrate stability. *Geochim. Geophys. Geosyst.* **17**, 3882–3892 (2016).

40. D. A. Wiesenburg, N. L. Guinasso Jr., Equilibrium solubilities of methane, carbon monoxide, and hydrogen in water and sea water. *J. Chem. Eng. Data* **24**, 356–360 (1979).

**Acknowledgments:** We thank B. Kopplin, M. Fleming, and A. Schwartz of the R/V *Ukpiagik* for providing skillful assistance of our science in Prudhoe Bay. We are grateful to M. Leonte for running GC-FID hydrocarbon concentration analyses in the Kessler laboratory. K.J.S. thanks A. Andersson of Stockholm University for fruitful discussions. **Funding:** The National Science Foundation (PLR-1417149; awarded to J.D.K.) primarily supported this work with additional support provided by the U.S. Department of Energy (DE-FE0028980; awarded to J.D.K.). Atmospheric  $^{14}\text{C-CH}_4$  measurements were funded by NASA via the Jet Propulsion Laboratory (Earth Ventures project “Carbon in Arctic Reservoirs Vulnerability Experiment”) to the University of Colorado under contract 1424124. K.M.S. acknowledges support from the University of Minnesota Grant-in-Aid program. **Author contributions:** K.J.S. and J.D.K. led the study and drafted the manuscript, with contributions from C.D.R. Fieldwork in Prudhoe Bay was performed by K.J.S., J.D.K., F.G.-T., and K.M.S. Dissolved  $^{14}\text{C-CH}_4$  samples were prepared by

K.J.S. and analyzed by J.R.S. Samples for  $^{14}\text{C}$ -DIC,  $^{14}\text{C}$ -DOC, atmospheric  $^{14}\text{C}$ -CH<sub>4</sub>, and atmospheric  $^{14}\text{C}$ -CO<sub>2</sub> analyses were prepared by F.G.-T. and X.X., K.M.S., J.B.M. and S.J.L., and X.X., respectively. Any use of trade, firm, or product names is for descriptive purposes only and does not imply endorsement by the U.S. government. **Competing interests:** The authors declare that they have no competing interests. **Data and materials availability:** All data needed to evaluate the conclusions in the paper are present in the paper and/or the Supplementary Materials. The water column data are also available at doi:10.18739/A2B69R. Additional information is available from the authors upon request.

Submitted 26 July 2017  
Accepted 13 December 2017  
Published 17 January 2018  
10.1126/sciadv.aa04842

**Citation:** K. J. Sparrow, J. D. Kessler, J. R. Southon, F. Garcia-Tigreros, K. M. Schreiner, C. D. Ruppel, J. B. Miller, S. J. Lehman, X. Xu, Limited contribution of ancient methane to surface waters of the U.S. Beaufort Sea shelf. *Sci. Adv.* **4**, eaao4842 (2018).

## Limited contribution of ancient methane to surface waters of the U.S. Beaufort Sea shelf

Katy J. Sparrow, John D. Kessler, John R. Southon, Fenix Garcia-Tigreros, Kathryn M. Schreiner, Carolyn D. Ruppel, John B. Miller, Scott J. Lehman and Xiaomei Xu

Sci Adv 4 (1), eaao4842.  
DOI: 10.1126/sciadv.aao4842

ARTICLE TOOLS

<http://advances.sciencemag.org/content/4/1/eaao4842>

SUPPLEMENTARY MATERIALS

<http://advances.sciencemag.org/content/suppl/2018/01/12/4.1.eaao4842.DC1>

REFERENCES

This article cites 40 articles, 2 of which you can access for free  
<http://advances.sciencemag.org/content/4/1/eaao4842#BIBL>

PERMISSIONS

<http://www.sciencemag.org/help/reprints-and-permissions>

Use of this article is subject to the [Terms of Service](#)